Controlling dynamic instability of three-level atoms inside an optical ring cavity

Wenge Yang,[1,2] Amitabh Joshi,[1] and Min Xiao[1,2,*]
[1]*Department of Physics, University of Arkansas, Fayetteville, Arkansas 72701, USA*
[2]*Microelectronics-Photonics Program, University of Arkansas, Fayetteville, Arkansas 72701, USA*
(Received 18 February 2004; published 22 September 2004)

Dynamic instability in the transmission field of an optical ring cavity containing three-level Λ-type rubidium atoms is studied in detail both experimentally and theoretically. The onset and periodicity of such dynamic oscillations in the cavity field can be controlled by the experimental parameters, such as intensity and frequency detuning of the coupling field and/or cavity field. Such nonlinear dynamic behavior is caused by competition between optical saturation of the cavity field and optical population pumping by the coupling field in the three-level atomic system.

DOI: 10.1103/PhysRevA.70.033807 PACS number(s): 42.65.Pc, 42.65.Sf, 42.50.Gy

I. INTRODUCTION

Dynamic instability was observed and carefully studied in the upper branch of the optical bistability (OB) curve in a system with two-level sodium atoms inside an optical cavity [1]. This dynamic effect was attributed to the mechanism known as Ikeda instability [2], which appears in analyzing the stability of the steady states in OB curves, assuming a medium response time much faster than the cavity round trip time. In this limit and under certain parametric conditions, a sequence of period doubling bifurcation leading to a region of apparently aperiodic dynamic oscillation was observed. Multimode instabilities as well as oscillatory instabilities leading to optical turbulence in the OB from a two-level atomic system were also reported [3]. The off-resonant-mode instability in mixed absorptive-dispersive optical bistability was studied and it was shown that a portion of the lower transmission branch could also be unstable in addition to the upper-branch instability found in the system with pure absorptive bistability [4]. The observation of instability due to the onset of the cavity side mode was reported in a bistable optical system with a homogeneously broadened two-level medium [5]. Other kinds of self-oscillation and instability were also observed using different two-level atomic systems inside an optical resonator [6]. All the above mentioned theoretical modelings and experimental observations were carried out in two-level atomic systems. A different kind of dynamic instability was observed in the transmission field of an optical cavity consisting of a cold cloud of cesium atoms [7]. In this system the degenerate Zeeman sublevels of the $6S_{1/2}$ $F=4$ and $6P_{3/2}$ $F'=5$ states interact with two cavity fields pumped by one input circularly polarized laser beam. The instability was considered to be caused by competition between optical pumping to the state $6S_{1/2}$ $F=4$, $m_F=4$ from all other Zeeman sublevels and optical saturation of the transition from the state $6S_{1/2}$ $F=4$, $m_F=4$ to the state $6P_{3/2}$ $F'=5$, $m_{F'}=5$. The observed oscillatory behavior in the cavity output field was modeled as a quasi-two-level system interacting with one cavity field and only qualitative comparison was made between the observed phenomenon and a simplified theoretical model [7]. The complexities in that system are mainly caused by the degenerate Zeeman sublevels involved and the trapping and the repumping laser beams for creating the cold atomic cloud. The major limitation of that experiment was the use of only one cavity input (circularly polarized) beam to provide both linearly polarized optical pumping and probing (or saturation) beams, which prevented the two competing physical processes from being independently adjusted to systematically study the dynamic instability.

Recently, we have experimentally observed similar dynamic instability in a system consisting of three-level atoms inside an optical cavity, as shown in Fig. 1, and demonstrated dependence of such dynamic behaviors on the intensity of

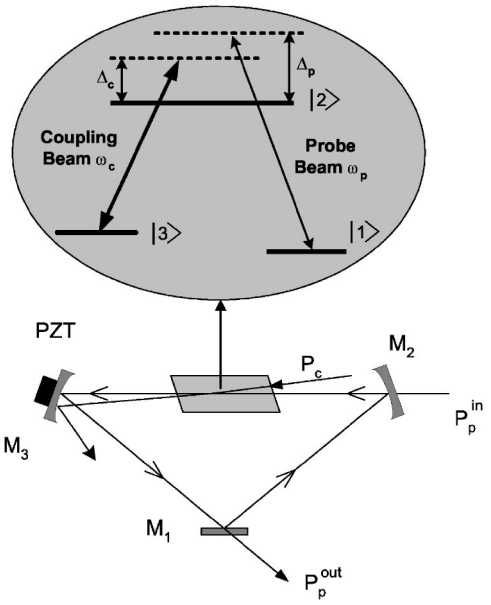

FIG. 1. Sketch of a three-level Λ-type atomic system and the optical ring cavity. M_1, M_2, and M_3 are mirrors; PZT is a piezoelectric transducer; $\Delta_c=\omega_c-\omega_{23}$, and $\Delta_p=\omega_p-\omega_{21}$ are the coupling and probe frequency detunings, respectively; P_c is the coupling laser beam; P_p^{in},P_p^{out} are the input and output probe laser beams, respectively.

*Corresponding author. Electronic address: mxiao@uark.edu

the cavity input field and the intensity of the coupling laser beam (which does not circulate inside the optical cavity) [8]. While such experimental demonstration clearly shows the competing processes between the optical pumping from level $|3\rangle$ to level $|1\rangle$ by the coupling beam and the optical saturation in the transition from level $|1\rangle$ to level $|2\rangle$ by the cavity (probe) field, no theoretical model was developed at that time to provide quantitative comparisons between theoretical calculations and the experimentally observed results. In this paper, we further investigate the behaviors of this interesting dynamic instability as functions of other experimental parameters, such as frequency detunings of the coupling and the probe laser beams. We have also developed an appropriate theoretical model to describe the full dynamics of the three-level atoms (through density matrix equations) interacting with two independent laser fields. The validity of assuming this three-level Λ-type electromagnetically induced transparency (EIT) system in view of the involved Zeeman sublevels has been well established both experimentally [9] and theoretically [10]. Quantitative comparisons between the theoretically simulated results and the experimentally observed behaviors are made and good agreements have been obtained. With the better known absorption [9], dispersion [11], and nonlinear [12] properties of such three-level EIT systems, the dynamic behaviors of three-level atoms inside an optical cavity can be well understood and controlled.

Although phenomena related to optical dynamic instability in various atomic systems have been studied for the past two decades, these observed dynamic effects do not have any experimental control. Our current system of three-level atoms inside an optical ring cavity has many advantages. The first one is the ability to independently control the frequencies and intensities of the coupling beam and the probe beam over large parameter ranges. Such tunability allows systematic studies of the competing optical pumping and optical saturation processes, and makes it possible to have quantitative comparisons between experimentally measured data and theoretically simulated results. Second, due to the reduced absorption [9], increased dispersion [11], and greatly enhanced nonlinearity [12] in such a three-level EIT system, the optical dynamic oscillation can be observed at much lower intensities and with much more sensitive dependence on the frequency detunings and intensities of the laser beams. Another advantage is the use of a two-photon Doppler-free configuration in the three-level atomic system [9], so an atomic vapor cell can be used inside the optical cavity instead of an atomic beam or cold atomic sample, which greatly simplifies the experimental setup and operation. Also, recent advances in demonstrating EIT-related effects have fueled renewed interest in optical dynamic effects in multilevel atomic systems, which will have potential impacts on applications of EIT in all-optical switching, all-optical buffering, and optical soliton generation. In view of these advancements the controllability of such optical dynamic effects becomes particularly important.

The theoretical model is described in Sec. II with predicted dynamic oscillations in the cavity transmission profile. The experimental setup and procedures are presented in Sec. III. In Sec. IV, quantitative comparisons are made between the theoretical simulations and experimentally measured results. A detailed discussion is given. Section V serves as a summary for the findings of this paper.

II. THEORETICAL MODEL

We consider a system with N three-level Λ-type atoms inside an optical ring cavity, as shown in Fig. 1. Our theoretical model is based on the density-matrix equations for three-level atoms together with the modified Maxwell equation for the cavity field (i.e., input-output field relationship equation). A coupling laser of frequency ω_c near the ω_{23} resonance couples levels $|2\rangle$ and $|3\rangle$, while a probe beam (which circulates inside the optical ring cavity as the cavity field) with frequency ω_p near the ω_{21} resonance couples level $|2\rangle$ and $|1\rangle$. Using standard techniques (see, e.g., [13]), the following equations for the three-level atomic system can be derived for the density-matrix elements under the rotating wave approximation:

$$\dot{\rho}_{11} = \gamma_{31}(\rho_{33} - \rho_{11}) + \gamma_{21}\rho_{22} - \frac{i}{2}\Omega_p^*\rho_{21} + \frac{i}{2}\Omega_p\rho_{21}^*, \quad (1a)$$

$$\dot{\rho}_{22} = -(\gamma_{23} + \gamma_{21})\rho_{22} - \frac{i}{2}\Omega_p\rho_{21}^* + \frac{i}{2}\Omega_p^*\rho_{21} - \frac{i}{2}\Omega_c\rho_{23}^* + \frac{i}{2}\Omega_c^*\rho_{23}, \quad (1b)$$

$$\dot{\rho}_{33} = \gamma_{31}(\rho_{11} - \rho_{33}) + \gamma_{23}\rho_{22} - \frac{i}{2}\Omega_c^*\rho_{23} + \frac{i}{2}\Omega_c\rho_{23}^*, \quad (1c)$$

$$\dot{\rho}_{21} = -(\gamma_{21} - i\Delta_p)\rho_{21} + \frac{i}{2}\Omega_p(\rho_{22} - \rho_{11}) - \frac{i}{2}\Omega_c\rho_{31}, \quad (1d)$$

$$\dot{\rho}_{23} = -(\gamma_{23} - i\Delta_c)\rho_{23} + \frac{i}{2}\Omega_c(\rho_{22} - \rho_{33}) - \frac{i}{2}\Omega_p\rho_{31}^*, \quad (1e)$$

$$\dot{\rho}_{31} = -[\gamma_{31} - i(\Delta_p - \Delta_c)]\rho_{31} + \frac{i}{2}\Omega_p\rho_{23}^* - \frac{i}{2}\Omega_c^*\rho_{21}, \quad (1f)$$

where $\Delta_p = \omega_p - \omega_{21}$ and $\Delta_c = \omega_c - \omega_{23}$ are probe and coupling frequency detunings, respectively. γ_{21} is the decay rate from level $|2\rangle$ to $|1\rangle$ and γ_{23} is the decay rate from level $|2\rangle$ to $|3\rangle$. γ_{31} denotes the nonradiative decay rate between the two ground levels $|3\rangle$ and $|1\rangle$. γ is defined as $\gamma \equiv (\gamma_{21} + \gamma_{23} + \gamma_{31})/2$. The laser linewidths $\delta\omega_p$ and $\delta\omega_c$ for the probe beam and coupling beam (considered as Lorentzian line shapes) can be taken into account by placing them in the decay rates as $\gamma \rightarrow \gamma + \delta\omega_p$, $\gamma_{31} \rightarrow \gamma_{31} + \delta\omega_p + \delta\omega_c$ [9]. Ω_p and Ω_c are the complex Rabi frequencies associated with the probe and coupling beams, respectively, defined as $\Omega_p = -d_{21}E_p/\hbar$ and $\Omega_c = -d_{23}E_c/\hbar$. d_{21} is the dipole matrix element between levels $|2\rangle$ and $|1\rangle$ and d_{32} is the dipole matrix element between levels $|2\rangle$ and $|3\rangle$. E_p and E_c are the complex probe and coupling field strengths, respectively.

In what follows we use α ($|\alpha|^2$ is the average photon flow, expressed in units of number of photons per second) to de-

note the field, which is related to the field strength E by

$$E_p = \sqrt{\frac{\hbar\omega_p}{2n\epsilon_0 c S_p}}\ \alpha_p, \tag{2a}$$

$$E_c = \sqrt{\frac{\hbar\omega_c}{2n\epsilon_0 c S_c}}\ \alpha_c, \tag{2b}$$

where ϵ_0 is the free-space permittivity and c is the speed of light in vacuum; S_p and S_c are the areas of the transverse sections of the probe and coupling light beams, respectively. In terms of α the complex Rabi frequencies of the probe and coupling beams become

$$\Omega_p = -\frac{d_{21}}{\hbar}\sqrt{\frac{\hbar\omega_p}{2n\epsilon_0 c S_p}}\ \alpha_p \equiv -2x_p\alpha_p, \tag{3a}$$

$$\Omega_c = -\frac{d_{23}}{\hbar}\sqrt{\frac{\hbar\omega_c}{2n\epsilon_0 c S_c}}\ \alpha_c \equiv -2x_c\alpha_c, \tag{3b}$$

where x_p and x_c are two constants introduced for simplicity. The probe laser circulates inside the optical cavity so α_p is a complex variable, which can be expressed as $\alpha_p = \alpha_1 + i\alpha_2$. The coupling laser is misaligned slightly from the probe laser axis, so it does not circulate inside the cavity. Without loss of generality, we can assume α_c to be real.

We further introduce the following real variables for the atomic density elements:

$$w_p = \rho_{22} - \rho_{11}, \tag{4a}$$

$$w_c = \rho_{22} - \rho_{33}, \tag{4b}$$

$$\rho_{21} = (u_{21} - iv_{21})/2, \tag{4c}$$

$$\rho_{23} = (u_{23} - iv_{23})/2, \tag{4d}$$

$$\rho_{31} = (u_{31} - iv_{31})/2, \tag{4e}$$

where w_p is the population inversion between level $|2\rangle$ and level $|1\rangle$ and w_c is the population inversion between level $|2\rangle$ and level $|3\rangle$. u_{ij} and v_{ij} are the real and imaginary parts of the corresponding matrix elements of the atomic density operator $\rho_{ij}(i \neq j)$. According to the definitions of w_p and w_c, plus the additional closeness or trace condition of $\rho_{11}+\rho_{22}+\rho_{33}=1$, we can get the following relations:

$$\rho_{22} = \frac{1 + w_p + w_c}{3}, \tag{5}$$

$$\rho_{33} - \rho_{11} = w_p - w_c. \tag{6}$$

Then we can easily rewrite the three-level Bloch equations for the atomic system from Eq. (1) as

$$\dot{w}_p = -\frac{\gamma_{23} + 2\gamma_{21}}{3}(1 + w_p + w_c) - \gamma_{31}(w_p - w_c) - 2x_p(\alpha_1 v_{21} + \alpha_2 u_{21}) - x_c\alpha_c v_{23}, \tag{7a}$$

$$\dot{w}_c = -\frac{2\gamma_{23} + \gamma_{21}}{3}(1 + w_p + w_c) + \gamma_{31}(w_p - w_c) - x_p(\alpha_1 v_{21} + \alpha_2 u_{21}) - 2x_c\alpha_c v_{23}, \tag{7b}$$

$$\dot{u}_{21} = -\gamma u_{21} + \Delta_p v_{21} + 2x_p\alpha_2 w_p + x_c\alpha_c v_{31}, \tag{7c}$$

$$\dot{v}_{21} = -\gamma v_{21} - \Delta_p u_{21} + 2x_p\alpha_1 w_p - x_c\alpha_c u_{31}, \tag{7d}$$

$$\dot{u}_{23} = -\gamma u_{23} + \Delta_c v_{23} - x_p(\alpha_1 v_{31} + \alpha_2 u_{31}), \tag{7e}$$

$$\dot{v}_{23} = -\gamma v_{23} - \Delta_c u_{23} + 2x_c\alpha_c w_c - x_p(\alpha_1 u_{31} - \alpha_2 v_{31}), \tag{7f}$$

$$\dot{u}_{31} = -\gamma_{31} u_{31} + (\Delta_p - \Delta_c)v_{31} + x_c\alpha_c v_{21} + x_p(\alpha_1 v_{23} + \alpha_2 u_{23}), \tag{7g}$$

$$\dot{v}_{31} = -\gamma_{31} v_{31} - (\Delta_p - \Delta_c)u_{31} - x_c\alpha_c u_{21} + x_p(\alpha_1 u_{23} - \alpha_2 v_{23}). \tag{7h}$$

Next, we derive the equation that governs the behavior of the probe field α_p, which circulates inside the cavity as the intracavity field. The change of the intracavity probe field α_p on a round trip time duration τ is due to the driving field α_p^{in} entering through the laser mirror M_2 with a transmission coefficient t_2, to the cavity decay γ_{cav} (due to the losses of the intracavity medium and the finite transmissions of the mirrors), and to the round trip phase shift Φ_{cav}:

$$\tau\frac{d\alpha_p}{dt} = t_2\alpha_p^{in} - \gamma_{cav}\alpha_p + i\Phi_{cav}\alpha_p. \tag{8}$$

This equation describes the mean field evolution of the probe beam over time intervals long compared to the cavity round trip time. The total round trip phase shift in the cavity has four contributions. The first part Φ_0 is simply the phase shift of the field propagating in the free space of the cavity. It is proportional to the geometrical length of the cavity and can be expressed as

$$\Phi_0 = kL = \frac{2\pi}{\lambda}(L_0 + v_{cav}t), \tag{9}$$

where L and L_0 are the instant and initial cavity lengths, respectively, and v_{cav} is the cavity scanning speed. If we assume the cavity to be initially on resonance with the field, the effect due to L_0 can be ignored and Φ_0 simply changes linearly with time. In the second part of the round trip phase shift, there are two contributions due to the presence of the atomic medium in the cavity; i.e., a linear phase shift and a nonlinear phase shift, which can be calculated through the first order and third order susceptibilities of the atomic system. For three-level Λ-type atoms and under the condition that the coupling field is much stronger than the probe field, these first and third order susceptibilities can be derived through a successive approximation method as [14]

$$\chi^{(1)} = \frac{iN|d_{21}|^2}{\epsilon_0 \hbar} \frac{1}{Y}\left(1 - \frac{2\gamma_{31}}{2\gamma + \gamma_{21}}\right) \tag{10}$$

and

$$\chi^{(3)} = -\frac{iN|d_{21}|^4}{3\epsilon_0 \hbar^3} \frac{1}{(2\gamma + \gamma_{21})} \frac{1}{Y}\left(\frac{1}{Y} + \frac{1}{Y^*}\right), \tag{11}$$

where N is the temperature-dependent atomic density function given in [15], and Y is defined as

$$Y \equiv \gamma_{21} - i\Delta_p + \frac{|\Omega_c|^2/4}{\gamma_{31} - i(\Delta_p - \Delta_c)}. \tag{12}$$

The linear and nonlinear phase shifts are proportional to the real parts of $\chi^{(1)}$ and $|E_p|^2\chi^{(3)}$, respectively, i.e., $\Phi_L \propto \mathrm{Re}[\chi^{(1)}]$ and $\Phi_{NL} \propto \mathrm{Re}[\chi^{(3)}]$. The nonlinear phase shift also depends on the intensity of the intracavity field $|E_p|^2$ [or $|\alpha_p|^2$ by the relation of Eq. (2)]. From Eq. (12) one can see that $\chi^{(1)}$ and $\chi^{(3)}$ depend on three parameters Δ_c, Δ_p, and Ω_c (which depends on the coupling laser power P_c). For simplicity, we write $\Phi_L \equiv e(\Delta_c, \Delta_p, P_c)$ and $\Phi_{NL} \equiv f(\Delta_c, \Delta_p, P_c)|\alpha_p|^2$, where e and f are two quantities depending on Δ_c, Δ_p, and P_c. When the condition of strong coupling field is not satisfied, we will use the general density-matrix Eqs. (1) to evaluate the nonlinear susceptibility in calculating the phase shift.

The last contribution to the round trip phase shift Φ_p comes from the interaction of atoms with the cavity field. It originates from the change in the population of the excited-state level and can be expressed as

$$\Phi_p = \tfrac{2}{3}(1 + w_c + w_p)\Phi_L. \tag{13}$$

The total phase shift in the cavity is then given by

$$\begin{aligned}\Phi_{cav} &= \Phi_0 + \Phi_L + \Phi_{NL} + \Phi_p \\ &= \frac{2\pi}{\lambda} v_{cav} t + \left(1 + \frac{2}{3}(1 + w_p + w_c)\right)e + f|\alpha_p|^2. \end{aligned} \tag{14}$$

The phase shift given by Eq. (14) considers only the dispersive interaction of fields with atoms and the absorption effect has been neglected. This is justified by the fact that under small frequency detuning the absorption coefficient experienced by the probe laser beam is nearly zero due to the EIT effect [9], while in the large detuning limit the phase shift due to absorption can be expressed as $\Phi_a \propto 1/\Delta_p^2$ [16], which is very small compared with the linear phase shift $\Phi_L \propto 1/\Delta_p$ and nonlinear phase shift $\Phi_{NL} \propto \alpha_p^2/\Delta_p^3$ and can also be neglected.

In terms of its real and imaginary parts α_1 and α_2, the equation for the cavity field α_p can be reformulated as

$$\begin{aligned}\tau\dot{\alpha}_1 = t_2\alpha_p^{in} - \gamma_{cav}\alpha_1 - \frac{2\pi}{\lambda} v_{cav} t\alpha_2 - \left(1 + \frac{2}{3}(1 + w_p + w_c)\right)e\alpha_2 \\ - f(\alpha_1^2 + \alpha_2^2)\alpha_2, \end{aligned} \tag{15a}$$

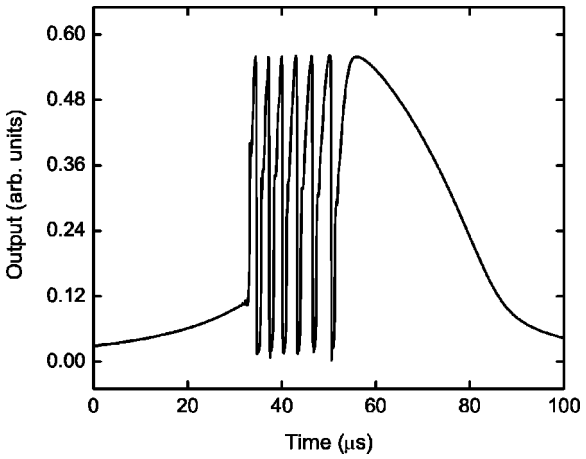

FIG. 2. Typical calculated cavity transmission profile. The parameters used in this calculation are $P_c = 10$ mW, $P_p^{in} = 2$ mW, $\Delta_c = 0$, and $\Delta_p = 30$ MHz.

$$\begin{aligned}\tau\dot{\alpha}_2 = -\gamma_{cav}\alpha_2 + \frac{2\pi}{\lambda} v_{cav} t\alpha_1 + \left(1 + \frac{2}{3}(1 + w_p + w_c)\right)e\alpha_1 \\ + f(\alpha_1^2 + \alpha_2^2)\alpha_1. \end{aligned} \tag{15b}$$

The atomic equations (7) and the field equations (15) constitute the total model of our system with N three-level atoms inside the optical ring cavity. By solving these dynamic equations simultaneously, we have obtained dynamic oscillation in the cavity transmission profile, as shown in Fig. 2. The initial conditions and the values of some parameters used in the calculation are $w_p(0) = -1$, $w_c(0) = 0$, $u_{21}(0) = u_{23}(0) = u_{31}(0) = v_{21}(0) = v_{23}(0) = v_{31}(0) = 0$, $\alpha_1(0) = 6 \times 10^6$, $\alpha_2(0) = 0$, $\gamma_{cav} = 0.03$, $\gamma_{21} = \gamma_{23} = 3 \times 10^6$ Hz, $\gamma_{31} = 1.1 \times 10^6$ Hz, $\tau \approx 1.2$ ns, $t_2 = 0.17$ (corresponds to 3% intensity transmissivity), and $v_{cav} = 200$ μm/s. The above set of ten ordinary differential equations shows extreme stiffness at our experimental conditions so Gear's third order method with a variable step size is used to solve these equations. The appearance (and disappearance) of such dynamic oscillations and the oscillation period can be controlled by changing the system parameters, such as the power of the coupling beam (P_c) and cavity input field (P_p), as well as frequency detunings of the coupling and probe beams (Δ_c and Δ_p, respectively). Quantitative comparisons between the experimental measurements and the theoretical calculations as functions of various parameters will be given in Sec. IV.

Similar oscillation in the transmission profile of a cavity containing cold Cs atoms was observed previously and a simple model was developed to qualitatively describe the observed phenomenon [7]. In that experiment, one circularly polarized laser beam was injected into the optical cavity, which interacts with all the Zeeman sublevels of the $6S_{1/2}$ $F = 4$ and $6P_{3/2}$ $F' = 5$ states. The model in Ref. [7] describes a competition between optical pumping to state $6S_{1/2}$ $F = 4$, $m_F = 4$ from all other Zeeman sublevels and optical saturation of the transition from state $6S_{1/2}$ $F = 4$, $m_F = 4$ to state $6P_{3/2}$ $F' = 5$, $m_{F'} = 5$. To make a direct comparison between our model and the model used by Ref. [7], let us consider a

simple case in which only two-level atoms are considered and the frequency detuning of the input field is very large compared to the atomic decay rate, i.e., $\Delta_p \gg \gamma$. Under these conditions, the quantities responsible for linear phase shift e and the nonlinear phase shift f in our model become

$$e = Ng^2/\Delta_p, \tag{16}$$

$$f = -2Ng^4/\Delta_p^3, \tag{17}$$

where g is the coupling constant of the atoms with the field,

$$g^2 = \frac{d_{21}^2 \omega_p}{2\epsilon_0 \hbar S_p c}. \tag{18}$$

These results agree with the model used in Ref. [7], which can be considered as a special case of the more general model presented in this work. Our model not only incorporates the situation in which the frequency detuning is not so big compared with the atomic decay rate, but also deals with other parameters as well, such as the coupling power (through $|\Omega_c|^2$) and coupling frequency detuning (Δ_c), as a result of treating the coupling and probe fields independently in the three-level atomic system. Our theoretical treatment of the system with three-level atoms inside an optical ring cavity is quite general, which allows direct comparisons with our systematic experimental studies for the dependence of such dynamic effects on various experimental parameters. Also, this model can be used to investigate other dynamic effects, such as chaos and tunneling in this system.

Another kind of oscillation in cavity transmission is worth mentioning at this point. When an empty optical cavity is excited by an incident beam at wavelength λ and the cavity length is slowly scanned, the output field can show an oscillation, which is known as the cavity ringdown effect [17]. This cavity ringdown oscillation usually exists in long cavities with high finesse. By summing up all the wave components that have undergone multiple reflections, the electric field inside the resonator at any instant can be obtained and thus the oscillation period of the output field can be predicted [17]. This effect can be predicted by our previously derived model without the atomic medium, i.e.,

$$\tau \frac{d\alpha_p}{dt} = t_2 \alpha_p^{in} - \gamma_{cav}\alpha_p + i\frac{2\pi v_{cav}}{\lambda} t\alpha_p. \tag{19}$$

This simple equation can be solved both numerically and analytically. Ringdown oscillation can be obtained and the time difference between the first two oscillation dips can be measured through the $|\alpha_p|^2$ versus t plot. At $\gamma_{cav}=0.002$, $v_{cav}=3600$ μm/s, $\lambda=795$ nm, and $L_0=36.5$ cm, the calculated period turns out to be 0.3 μs, which exactly matches the result obtained in Ref. [17]. To avoid confusion between this cavity ringdown effect in an empty cavity and the observed optical dynamic oscillation in our experiment due to nonlinear dynamic effects in the three-level atomic medium, we make the following comments. First, in order to observe the cavity ringdown effect, the cavity needs to have very high finesse, or equivalently the cavity decay γ_{cav} should be very small. For the above calculation, the cavity ringdown oscillation disappears when γ_{cav} is increased to 0.008 (equivalent to a cavity finesse of 400). The value of cavity decay in our experiment is much higher than this, so we cannot observe this ringdown effect in our experiment. Second, the ringdown oscillation quickly disappears within the time scale of only several microseconds after the cavity input laser is turned on. Normally we are not interested in this transient time region so we can just ignore this initial oscillation. Third, in order to observe the cavity ringdown oscillation, the cavity length needs to be scanned at a very fast speed (3600 μm/s in the above example, which is much bigger than the one used in our experiment). Finally, the periods of such cavity ringdown oscillations are usually much smaller than the values predicted for the optical dynamic oscillation in our system.

III. EXPERIMENTAL MEASUREMENTS

Our basic experimental setup is shown in Fig. 3. The energy levels of the three-level Λ-type system in the D_1 line of ^{87}Rb atom are shown in the bubble of Fig. 1. The optical ring cavity is about 36.5 cm long and is composed of three mirrors. The flat mirror M_1 and the concave mirror M_2 ($R=10$ cm) have about 1% and 3% transmissivities, respectively, while the third mirror M_3 is concave ($R=10$ cm) with a reflectivity larger than 99.5% and is mounted on a piezoelectric transducer (PZT). The cavity decay γ_{cav} is estimated to be around 0.03 assuming a lossless intracavity medium. The empty cavity finesse was measured to be about 100 with a free spectral range of 822 MHz. The rubidium vapor cell is 5 cm long with Brewster windows and is wrapped in μ metal for magnetic shielding, as well as heat tape for atomic density control. The experiment was conducted at a vapor cell temperature of about 70°C. The probe laser beam enters the cavity through mirror M_2 and circulates inside the cavity as the cavity field. Another laser beam, i.e., the controlling or coupling beam, is introduced through the polarizing beam splitter (PBS) with an orthogonal polarization to the probe beam. The coupling beam is misaligned from the cavity axis slightly (about 2° angle) so that it does not circulate inside the ring cavity. The cavity is mode matched to the probe beam using a lens with 15 cm focal length. The radii of the coupling beam and the cavity field at the center of the Rb vapor cell are estimated to be 700 μm and 80 μm, respectively. Due to the insertion losses of the PBS and reflection losses from the vapor cell windows, the cavity finesse is degraded to about 45 at a frequency far from atomic resonance. A third laser beam is introduced into the cavity through mirror M_3, which is used to lock the cavity and its frequency is tuned far from the probe and coupling lasers to avoid affecting the experiment. The probe input intensity of the cavity is controlled by PBS2 and a half-wave plate between the Farady rotator and the cavity. The coupling input intensity is also controlled in a similar manner by PBS4 and a half-wave plate.

Both the probe and coupling lasers are extended cavity diode lasers. The coupling laser is tuned to the $5S_{1/2}$ $F=2 \leftrightarrow 5P_{1/2}$ $F'=2$ transition, while the probe laser is tuned to the $5S_{1/2}$ $F=1 \leftrightarrow 5P_{1/2}$ $F'=2$ transition in ^{87}Rb. Both lasers are frequency locked to their respective Fabry-Pérot cavities

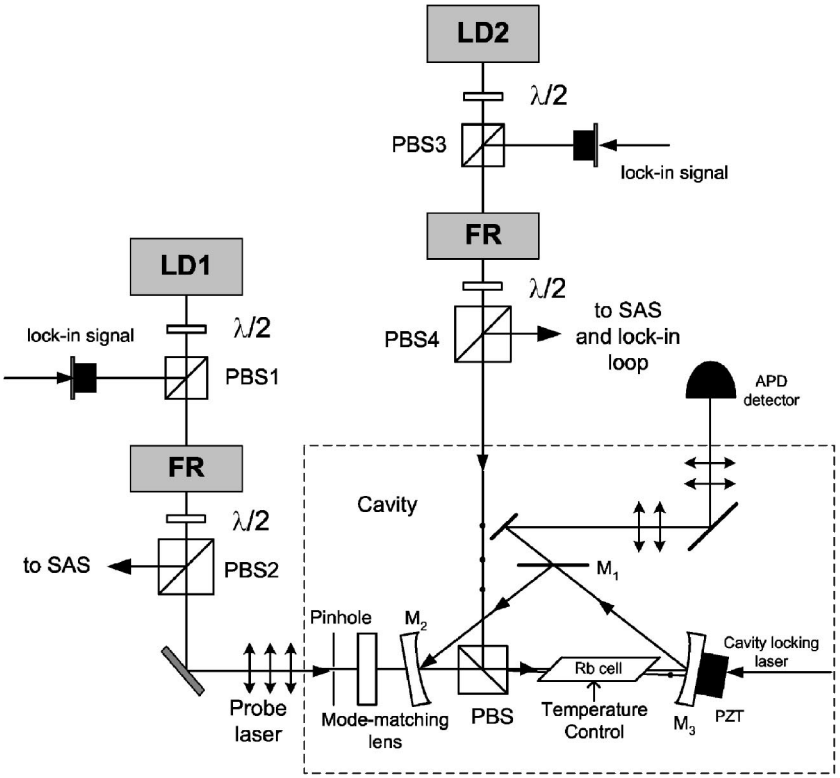

FIG. 3. Experimental setup. LD1 is the probe diode laser; LD2 is the coupling diode laser; PBS and PBS1–PBS4 are polarizing cubic beam splitters; $\lambda/2$ is the half-wave plate; M_1–M_3 are cavity mirrors; FR is a Faraday rotator; SAS is a saturation absorption spectroscopy used to monitor the probe frequency; and APD is the avalanche photodiode detector.

using our two-stage locking system, in which the first stage is to lock the laser frequency to one of the resonant frequencies of an external Fabry-Pérot cavity and the second stage is to slowly tune the output frequency to any desired value by changing the voltage applied to the PZT on which one of Fabry-Pérot cavity mirrors is mounted. Using this method, a detuning range in the order of several hundred megahertz can be achieved easily. The frequency detunings of lasers from their respective atomic transitions are set and monitored separately by using another Fabry-Pérot cavity. One of the key advantages of the current experimental system is the use of the two-photon Doppler-free configuration [9]. By propagating the coupling and probe laser beams collinearly through the vapor cell containing three-level Λ-type rubidium atoms, the first order Doppler effect is eliminated even in an atomic vapor cell, which greatly reduces the experimental complications.

The first step in the experiment is to lock the frequencies of both the coupling and the probe lasers. To achieve this, we first tune and lock the coupling beam to the resonant frequency of the coupling transition ($5S_{1/2}$, $F=2\rightarrow 5P_{1/2}$, $F'=2$). Then, we tune and lock the probe beam to the resonant frequency of the probe transition ($5S_{1/2}$, $F=1\rightarrow 5P_{1/2}$, $F'=2$). With both lasers frequency locked, we can slowly tune the applied voltages on the PZTs of the two Fabry-Pérot cavities to bring the laser output frequencies to any desired values. Then the length of the cavity is scanned across its resonance by applying a ramp voltage to the PZT mounted on mirror M_3. The cavity transmission is measured by an avalanche photodiode. Without the coupling beam, the cavity transmission profile is basically symmetric. When the coupling field is present, depending on the values of parameters, the cavity transmission profile becomes asymmetric or oscillatory due to dynamical instability. Such an asymmetric cavity transmission profile is caused by the enhanced Kerr nonlinearity in which the index of refraction of the atomic vapor is dependent on the intensity of the intracavity probe intensity as $n=n_0+n_2I_p$ [8]. This optical dynamic oscillation in the cavity transmission depends sensitively on the experimentally controllable parameters, such as intensity and frequency detuning of the coupling beam and intensity and frequency of the probe (cavity input) beam. We have made systematic experimental measurements of the dynamic instability as functions of these experimental parameters.

IV. COMPARISONS AND DISCUSSION

First, we present a qualitative comparison between the experimental observations and theoretical calculations of the optical dynamic oscillation in the cavity transmission. Figure 4 shows three experimental cavity transmission profiles (left column) and three corresponding theoretically calculated results (right column) for three different probe frequency detunings. The parameters used in the experimental measurements and theoretical calculations are $P_c=11$ mW, $P_p^{in}=2.8$ mW, and $\Delta_c=0$, with probe frequency detunings (a), (d) $\Delta_p=25$ MHz; (b), (e) $\Delta_p=35$ MHz; and (c), (f) $\Delta_p=45$ MHz. The cavity input power is measured just before it enters the cavity. One can clearly see that the theoretical calculations match quite well with the experimental results. The oscillation time period decreases with increasing probe frequency detuning, until the oscillation finally stops when the probe frequency detuning reaches $\Delta_p=60$ MHz (not shown here).

Next, we plot the measured oscillation period as a function of probe beam frequency detuning Δ_p, as shown in Fig.

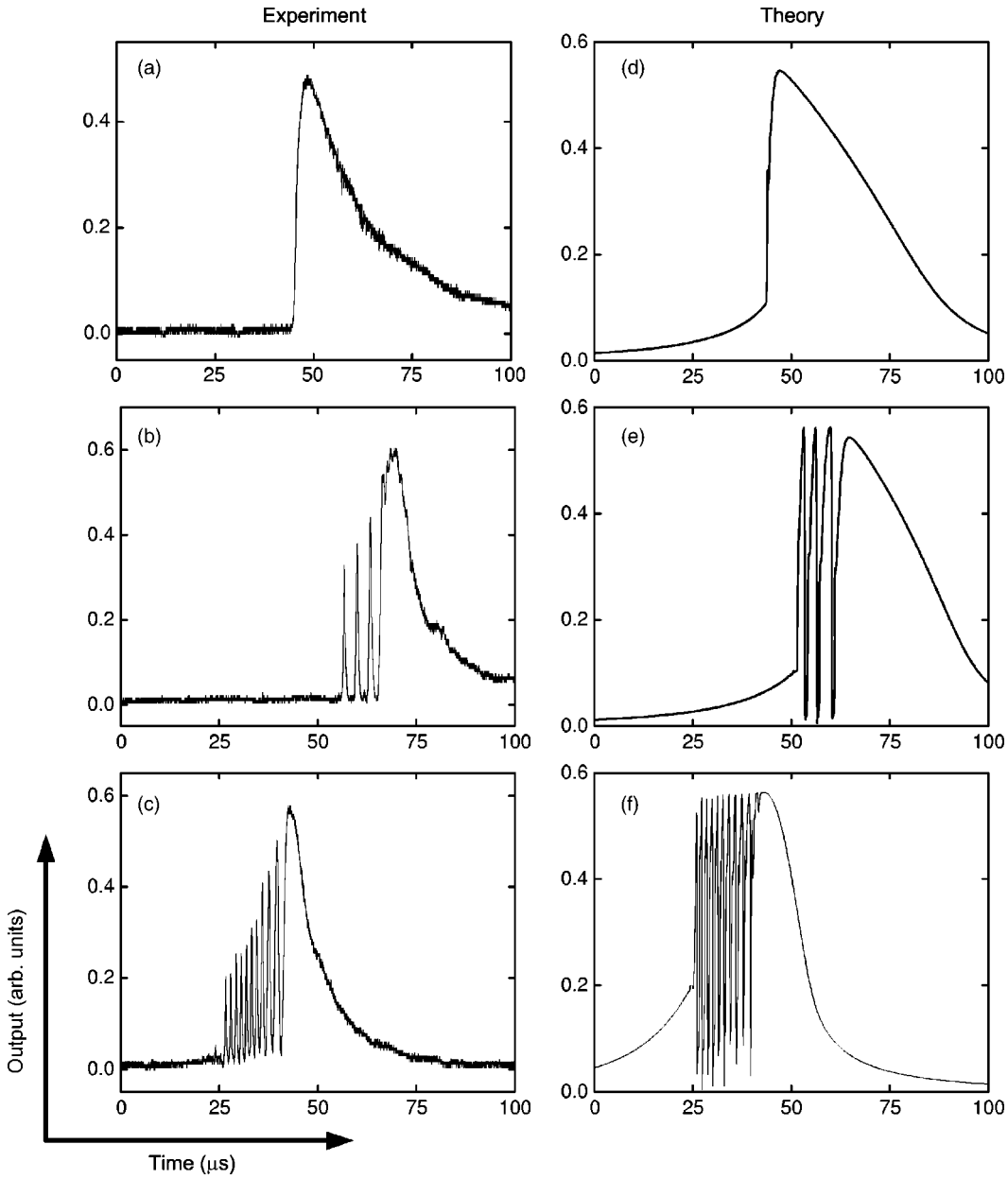

FIG. 4. Experimentally observed and theoretically calculated cavity transmission profiles from an optical ring cavity containing three-level Λ-type atoms for three different values of coupling frequency detuning. The left column is the experimental observations and the right column is the corresponding theoretical calculations. The parameters used in the experiment and theoretical calculation are $P_c=11$ mW, $P_p^{in}=2.8$ mW, $\Delta_c=0$, and (a), (d) $\Delta_p=25$ MHz; (b), (e) $\Delta_p=35$ MHz; (c), (f) $\Delta_p=45$ MHz.

5(a), together with the calculated theoretical curve. As one can see the agreement between the experimentally measured data and the theoretically calculated results is quite good. The parameters used for this plot are $\Delta_c=0$, $P_c=11.0$ mW, and $P_p^{in}=3.0$ mW for both the experimental measurement and theoretical calculation. The atomic number density used for the theoretical curve is $N=10^{10}/\mathrm{cm}^3$, corresponding to $T=70.3°\mathrm{C}$. Figure 5(b) plots the experimentally measured and theoretically calculated oscillation period as a function of coupling frequency detuning (Δ_c) with $\Delta_p=0$, $P_c=11.0$ mW, and $P_p^{in}=3.0$ mW. Figure 6(a) gives the measured oscillation period as a function of coupling beam power together with the theoretically calculated results. The parameters used for this plot are $\Delta_c=0$, $\Delta_p=35$ MHz, $P_p^{in}=3.0$ mW, and $T=70°\mathrm{C}$. Figure 6(b) presents the experimental and theoretical curves for the oscillation period versus cavity input power with $\Delta_c=0$, $\Delta_p=35$ MHz, $P_c=11.0$ mW, and $T=70°\mathrm{C}$. The experimental parameters were all measured directly and no fitting parameters are used for making such comparisons with the theoretical calculations.

The instability described here is caused by two competing dynamic processes in the system, i.e., optical pumping from state $5S_{1/2}$ $F=2$ to state $5S_{1/2}$ $F=1$ by the coupling field and the nonlinear saturation effect in the transition from state $5S_{1/2}$ $F=1$ to state $5P_{1/2}$ $F'=2$ due to the cavity field. The

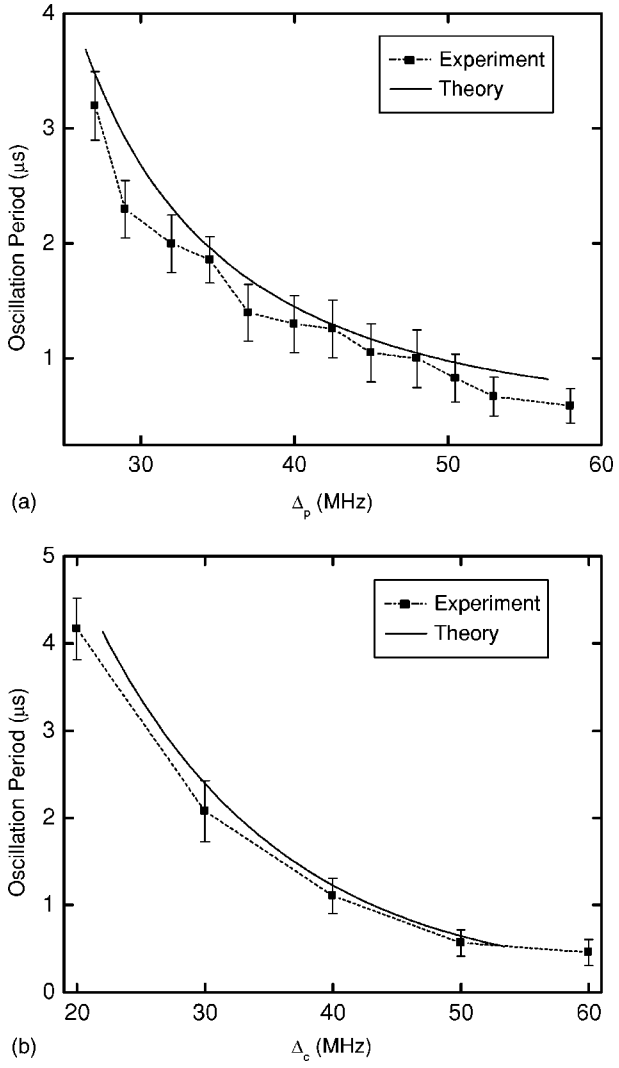

FIG. 5. Comparison between experimentally measured and theoretically calculated oscillation period versus (a) probe frequency detuning Δ_p and (b) coupling frequency detuning Δ_c. The parameters used for the plots are (a) $\Delta_c=0$, $P_c=11.0$ mW, and $P_p^{in}=3.0$ mW and (b) $\Delta_p=0$, $P_c=11.0$ mW, and $P_p^{in}=3.0$ mW for both the experiment and theoretical calculation.

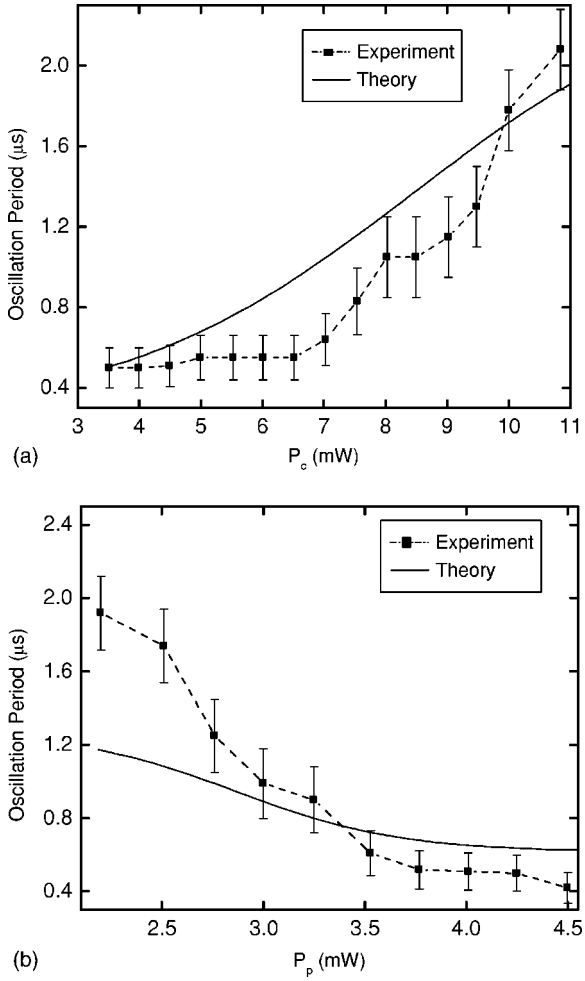

FIG. 6. Comparison between experimentally measured and theoretically calculated oscillation period versus (a) coupling power and (b) cavity (probe) power. The parameters used are (a) $\Delta_c=0$, $\Delta_p=35$ MHz, and $P_p^{in}=3.0$ mW, and (b) $\Delta_c=0$, $\Delta_p=35$ MHz, and $P_c=11.0$ mW for both experiment and theoretical calculation.

oscillation time period is determined by the relative strengths of these two dynamic processes, which are affected by the intensities and frequency detunings of the coupling and probe fields. A qualitative description of the oscillation behavior versus the coupling and probe input powers is given in Ref. [8]. Similar relations also exist for the probe and coupling frequency detunings, although they are not as straightforward as their dependences on the intensities of these two beams. The difference between the power and frequency detuning is that both frequency detunings play the same role while the probe and coupling powers play opposite roles, i.e., larger probe power increases the effect of nonlinear saturation while larger coupling power increases the effect of optical pumping, but both coupling and probe frequency detunings increase optical saturation. When the coupling frequency detuning increases, the strength of the optical pumping decreases, which effectively enhances the optical saturation process. The reason for increasing optical saturation with increasing probe frequency detuning lies in the typical EIT absorption behaviors, i.e., lower absorption at exact resonance due to EIT, but higher absorption with nonzero probe detuning [9]. These behaviors can be clearly seen from Fig. 5 and 6. The optical cavity plays an important role in the observed optical instability. It is the enhanced Kerr nonlinearity of the multilevel atomic medium due to induced atomic coherence [12] together with the feedback mechanism through the optical ring cavity that produce such optical dynamic instability behavior.

The relatively larger differences in the two curves of oscillation period versus probe power (Fig. 6) can be attributed to several factors. One is the neglected spatial distribution (Gaussian beam profile, focusing, and the propagation effect in the cell) of the cavity field in the theoretical calculation, which has a bigger impact for the intracavity field intensity and its interaction with the atoms. A second important issue is the uncertainty in experimentally determining the intracavity intensity from the cavity input power due to some inaccuracy in estimating the cavity field beam size. The third

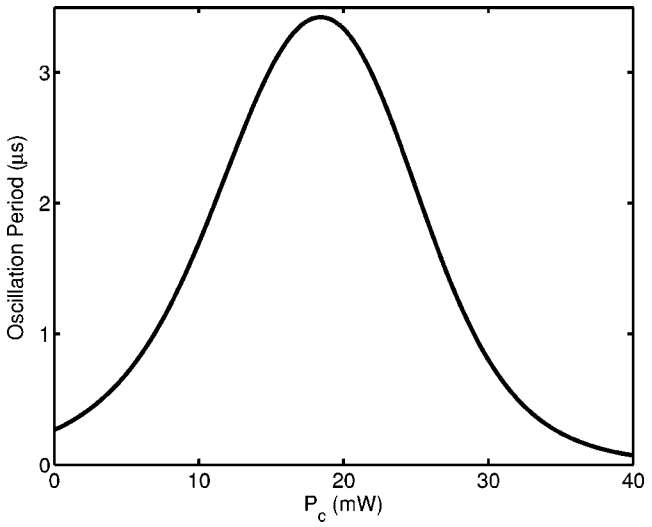

FIG. 7. Theoretical prediction of the oscillation period at higher coupling power level. The parameters used in this calculation are P_c=3 mW, Δ_c=0, and Δ_p=30 MHz.

factor is the error introduced by the discrepancy in the measured and calculated EIT absorption inside the cavity (a small difference in absorption can have a big effect in the saturation). Zeeman sublevels in the involved states contribute to the optical pumping effect, which has not been taken into account in the theoretical calculation. Another factor could be the exclusion of second order residual Doppler effect in this system [9]; it was not considered in the current calculation.

Currently our experiment is limited by the relatively low output power of the coupling laser (up to 12 mW delivered to the atomic vapor cell). Using our theoretical model, we can predict the oscillation behavior of the cavity transmission profile at higher coupling power levels, as shown in Fig. 7. One can see that the oscillation period increases initially up to a maximum value as the coupling power increases. When the coupling power reaches a certain value (around 18 mW), the oscillation period decreases toward zero with further increase in coupling power. In experimental measurements, the oscillation might disappear at such higher coupling power due to the imbalance in the competing processes as demonstrated in Ref. [8], so this oscillation period decrease with increasing coupling power might not be observed.

V. SUMMARY

We have experimentally observed and theoretically studied optical dynamic instability in a three-level Λ-type atomic system inside an optical ring cavity. The optical instability can be independently controlled by adjusting experimental parameters, such as the powers and frequency detunings of the coupling and cavity fields. Such control offers many advantages over the previous experimental system [7], where the experimental tunability is limited by the constraint of using only one laser beam to facilitate the two competing nonlinear processes. We developed an appropriate theoretical model to incorporate a three-level atomic system interacting with two independent laser beams, as well as the effects of other important controlling parameters such as the coupling power and coupling frequency detuning. We experimentally explored the optical instability behavior over large ranges of the parameter space, and the observations are found to be consistent with the theoretically calculated results of this model. These systematic studies of dynamic behaviors in such an interesting system of a three-level EIT medium inside an optical cavity can not only help our fundamental understanding of atom-cavity field interactions, but also provide useful information for potential applications of multilevel EIT systems in all-optical switches, all-optical buffering, and optical solitons, which are key elements for all-optical networking. Also, this general equations can be used to study other dynamic effects in such composite systems of three-level atoms inside an optical cavity, such as chaos, coherent transient effects, and tunneling.

ACKNOWLEDGMENTS

The contribution of Hai Wang in the early stage of this research work is acknowledged. We acknowledge funding support from the National Science Foundation and the Office of Naval Research.

[1] L. A. Orozco, A. T. Rosenberger, and H. J. Kimble, Phys. Rev. Lett. **53**, 2547 (1984); L. A. Orozco, H. J. Kimble, A. T. Rosenberger, L. A. Lugiato, M. L. Asquini, M. Brambilla, and L. M. Narducci, Phys. Rev. A **39**, 1235 (1989).
[2] K. Ikeda, Opt. Commun. **30**, 257 (1979); K. Ikeda, H. Daido, and O. Akimoto, Phys. Rev. Lett. **45**, 709 (1980).
[3] B. Ségard, B. Macke, L. A. Lugiato, F. Prati, and M. Brambilla, Phys. Rev. A **39**, 703 (1989); H. J. Carmichael, R. R. Snapp, and W. C. Schieve, *ibid.* **26**, 3408 (1982).
[4] M. L. Asquini, L. A. Lugiato, H. J. Carmichael, and L. M. Narducci, Phys. Rev. A **33**, 360 (1986).
[5] B. Ségard, W. Sergent, B. Macke, and N. B. Abraham, Phys. Rev. A **39**, 6029 (1989).
[6] W. J. Firth, R. G. Harrison, and I. A. Al-Saidi, Phys. Rev. A **33**, 2449 (1986); M. L. Berre, E. Ressayre, and A. Tallet, *ibid.* **43**, 6345 (1991).
[7] A. Lambrecht, E. Giacobino, and J. M. Courty, Opt. Commun. **115**, 199 (1995).
[8] H. Wang, D. J. Goorskey, and M. Xiao, Phys. Rev. A **65**, 011801(R) (2001).
[9] Y. Li and M. Xiao, Phys. Rev. A **51**, 4959 (1995); J. Gea-Banacloche, Y. Li, S. Jin, and M. Xiao, *ibid.* **51**, 576 (1995).
[10] H. Y. Ling, Y. Li, and M. Xiao, Phys. Rev. A **53**, 1014 (1996).
[11] M. Xiao, Y. Li, S. Jin, and J. Gea-Banacloche, Phys. Rev. Lett. **74**, 666 (1995).
[12] H. Wang, D. J. Goorskey, and M. Xiao, Phys. Rev. Lett. **87**,

073601 (2001); Opt. Lett. **27**, 258 (2002).
[13] M. O. Scully and M. S. Zubairy, *Quantum Optics* (Cambridge University Press, Cambridge, U.K., 1997).
[14] H. Wang, D. J. Goorskey, and M. Xiao, J. Mod. Opt. **49**, 335 (2002).
[15] A. S. Truscott, M. E.J. Friese, N. R. Heckenberg, and H. Rubinsztein-Dunlop, Phys. Rev. Lett. **82**, 1438 (1999).
[16] L. Hilico, C. Fabre, S. Reynaud, and E. Giacobino, Phys. Rev. A **46**, 4397 (1992).
[17] J. Poirson, F. Bretenaker, M. Vallet, and A. L. Floch, J. Opt. Soc. Am. B **14**, 2811 (1997); J. W. Hahn, Y. S. Yoo, J. Y. Lee, J. W. Kim, and H-W. Lee, Appl. Opt. **38**, 1859 (1999); K. An, C. Yang, R. R. Dasari, and M. S. Feld, Opt. Lett. **20**, 1068 (1995).